ACS APPLIED MATERIALS & INTERFACES

Research Article

www.acsami.org

Optical Regulation of Protein Adsorption and Cell Adhesion by Photoresponsive GaN Nanowires

Jingying Li,[†,∥] Qiusen Han,[†,∥] Ying Zhang,[†] Wei Zhang,[‡] Mingdong Dong,[§] Flemming Besenbacher,[§] Rong Yang,*[,†] and Chen Wang*[,†]

[†]CAS Key Lab for Biological Effects of Nanomaterials and Nanosafety, National Center for Nanoscience and Technology, Beijing 100190, People's Republic of China

[‡]Institute of Applied Physics and Computational Mathematics, P.O. Box 8009(28), Beijing 100088, People's Republic of China

[§]Interdisciplinary Nanoscience Center, Aarhus University, 8000 Aarhus C, Denmark

ABSTRACT: Interfacing nanowires with living cells is attracting more and more interest due to the potential applications, such as cell culture engineering and drug delivery. We report on the feasibility of using photoresponsive semiconductor gallium nitride (GaN) nanowires (NWs) for regulating the behaviors of biomolecules and cells at the nano/biointerface. The GaN NWs have been fabricated by a facile chemical vapor deposition method. The superhydrophobicity to superhydrophilicity transition of the NWs is achieved by UV illumination. Bovine serum albumin adsorption could be modulated by photoresponsive GaN NWs. Tunable cell detachment and adhesion are also observed. The mechanism of the NW surface responsible for modulating both of protein adsorption and cell adhesion is discussed. These observations of the modulation effects on protein adsorption and cell adhesion by GaN NWs could provide a novel approach toward the regulation of the behaviors of biomolecules and cells at the nano/biointerface, which may be of considerable importance in the development of high-performance semiconductor nanowire-based biomedical devices for cell culture engineering, bioseparation, and diagnostics.

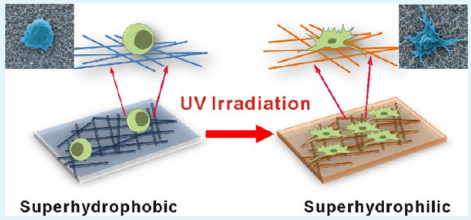

KEYWORDS: *protein adsorption, cell adhesion, semiconductor, gallium nitride, nanowire, nano/biointerface*

INTRODUCTION

Interfacing nanowires with living cells has received increased attention in the advances of biological applications of nanostructures.[1−6] Recent progress in this field includes drug delivery, biosensors, and biomedical implants, etc. Semiconductor nanowires, combining the properties of high aspect ratio and sufficient rigidity with the advantages of controllable electric properties and mature fabrication, could potentially be used as a powerful tool for investigating cell behaviors.[7,8] Yang and co-workers reported that cells could be cultured on vertical Si nanowire arrays. The nanoscale diameters of the wires allowed them to penetrate cells without cellular damage and require no external forces. Gene delivery using a Si nanowire array has already been demonstrated.[7]

Krivitsky et al. reported that by combining the Si nanowire-based separation device and Si nanowire sensor arrays into one platform, the protein biomarkers from blood samples could be detected with high sensitivity.[8] Qi et al. studied the interactions between LX-2 (human hepatic cell), HepG2 (human hepatoma cell line) cells, and Si nanowire arrays. They observed that Si nanowires could increase the cell-substrate adhesion force and, at the same time, restrict cell spreading.[9] Other groups also studied cell proliferation on Si and other semiconductor nanowires.[6,10−12]

It could be noted that a number of studies have engaged in the examination of the effects of various semiconductor nanowires on the biological functions of neuron cells. For example, Hällström et al. showed that peripheral sensory neurons and other cells from adult mouse dorsal root ganglia could adhere and proliferate on GaP nanowire substrates.[13] In addition, semiconductor nanowire-based neuron devices that could monitor or stimulate neurons with high sensitivity have also been recently reported for their great potential applications in neuroscience.[14−19]

Gallium nitride (GaN) is a photosensitive semiconductor material with direct and wide bandgap. GaN is well-known for its excellent optoelectronic properties, high mobility, and good thermal and chemical stability.[20−25] Such advantages make GaN good candidates for development of high-performance biomedical devices.[26−28]

Gebinoga et al. investigated the interaction between NG108-15 nerve cells and diisopropylfluorophosphate using the aluminum gallium nitride/gallium nitride (AlGaN/GaN) FET.[29]

Jewett et al.[30] studied the biocompatibility of GaN using the PC12 cell line, which is commonly used in modeling neural differentiation. Their results showed that GaN is a biocompatible material that could have potential applications in neuroscience. Young et al.[31] reported that rat cerebellar granule

Received: July 27, 2013
Accepted: September 17, 2013
Published: September 27, 2013

   dx.doi.org/10.1021/am403070g | *ACS Appl. Mater. Interfaces* 2013, 5, 9816−9822

neurons grew better on GaN than on silicon or polystyrene. GaN has also been used to study other neural cells.[32,33]

Since GaN nanowires (NWs) have much higher surface conductivity compared to the bulk GaN, they are promising candidates for applications of NW-based neuron devices with high quality.[13,34] It is therefore of great interest to gain insight into the interfacial properties between GaN NWs and living cells, which could facilitate an optimization of the relevant applications.

In this study, we report on the optically regulated protein adsorption and cell adhesion by photoresponsive GaN NWs. To the best of our knowledge, such optical regulation of biomolecule and cell behaviors in the nano/biointerface upon light stimulation has not been reported previously.

It is well-known that wettability and the chemical properties of the surface will greatly influence the protein adsorption and cell adhesion on a solid surface.[35−37] Besides the general studies on hydrophobic/hydrophilic surfaces, two extreme wettability ranges, superhydrophobic and superhydrophilic surfaces, have drawn more and more attention in biomedical research due to their potential importance.[38−41] Substantial effort is needed for the development of novel nanostructure-based switchable surfaces from superhydrophobic to superhydrophilic to meet increasing demand of many biomedical devices.

We have successfully fabricated GaN NWs by a facile and inexpensive chemical vapor deposition (CVD) method. The wettability of GaN NWs could be controlled by UV illumination. The bovine serum albumin (BSA) was selected for the protein adsorption study, which is of significant relevance to biocompatibility and drug delivery applications.[42] The NIH 3T3 and SH-SY5Y cell lines were chosen for modeling cell adhesion studies. The NIH 3T3 cell line has been widely used to study the interactions between the cells and the solid surfaces.[43] The neuroblastoma SH-SY5Y cell line was chosen for this study because it was commonly used as a model system in nerve cell studies.[44]

In this work, we will analyze the correlation between changes in wettability of GaN NWs upon light stimulation and the protein adsorption and cell adhesion. The experimental results show that the combination of the photoresponsive GaN surface and the magnification effect of micro/nanostructures result in a large-scale change of surface wettability from superhydrophobicity to superhydrophilicity by UV light stimuli, which subsequently modulate the protein adsorption and cell adhesion. These observations of the modulation effect on protein adsorption and cell adhesion could provide a novel approach toward regulating the behaviors of biomolecules in the nano/biointerface, which may be of considerable importance to both fundamental research and practical applications.

EXPERIMENTAL SECTION

Synthesis of GaN Nanowires. GaN NWs were synthesized by a typical CVD method. A quartz boat that contained a mixture of gallium, gallium oxide, and graphite was placed in the center of a tube furnace. The as-prepared substrate was put in the downstream of the furnace. N_2 was used as carrier gas at a flow rate of 40 sccm (standard cubic centimeter per minute). An additional flow of 20 sccm ammonia was introduced into the tube as reaction gas. The furnace temperature was increased to 960 °C and kept for 30 min for synthesis of GaN NWs. Then, the furnace was naturally cooled to room temperature with N_2 flowing continuously.

Characterization. The morphology of the as-prepared GaN NWs was studied with field-emission scanning electron microscope (Hitachi S-4800). The crystallographic information was established with the powder X-ray diffraction (Bruker D8). Transmission electron microscopy images were obtained by the transmission electron microscopy (Tecnai G2 F20) to confirm the structure of one single GaN NW. The wettability of the GaN NW surface was characterized by water contact angle using a contact-angle goniometer (DSA100). UV illumination was carried out using a Xe lamp (CEL-HX UV300) equipped with a 390 nm cutoff filter. The GaN samples before and after UV illumination were analyzed by X-ray photoelectron spectroscopy (XPS) using XPS spectrometer (ESCALAB 250Xi).

Protein Adsorption. Bovine serum albumin (BSA) (Sigma, 98%) was used as a model protein in this study. The experiments of BSA adsorption on the GaN surfaces with different wettabilities were performed by incubating the GaN substrates in BSA/PBS solution at pH 7.4 for 4 h. Protein concentrations were determined by using the micro-bicinchoninic acid (BCA, Sigma) assay according to the instructions of the manufacturer. The adsorbed protein amount on the sample surface was determined by subtracting the amount of protein in the solution.

Cell Culture. NIH 3T3 and SH-SY5Y cells were seeded on GaN NWs before and after UV irradiation. NIH 3T3 cells were cultured in DMEM medium (Hyclone) with 100 IU/mL penicillin, 100 μg/mL streptomycin, and 1% glutamine and supplemented with 10% (V/V) heat-inactivated calf serum (Gibco). SH-SY5Y cells were cultured in 1640 medium (Hyclone) with 10% (V/V) heat-inactivated fetal bovine serum (FBS, Sigma), 100 IU/mL penicillin, and 100 μg/mL streptomycin. The culture plates were placed in the incubator, which contains 5% CO_2. The temperature of the incubator was 37 °C.

Cell Study by Fluorescence Microscopy. NIH 3T3 and SH-SY5Y cells ($\sim 2 \times 10^4$ cells/ml) were cultured on different substrates that were placed in 24-well plates. After 48 h, the cells were stained with acridine orange (Sigma Aldrich), washed with PBS solution three times and studied under a fluorescence microscope (Leica, Germany) using a 515 nm pass filter. The number of cells on GaN NW surfaces was counted with three randomly taken images for each sample.

Immunostaining. First, the samples were washed with PBS solution after being cultured for 48 h; then they were fixed with 4% paraformaldehyde for 20 min and washed again. Second, the samples were permeabilized with PBST (0.1% Triton X-100 in PBS) for 10 min and washed with PBS three times. Third, cells were stained for vinculin, actin, and nucleus. Briefly, cells were incubated in mouse monoclonal antivinculin antibody (Sigma Aldrich), then donkey antimouse secondary antibody conjugated with Alexa Fluor 594 (Invitrogen) was added. At the same time, actin was stained with phalloidin conjugated with FITC (Sigma Aldrich). Nuclei were labeled with 4′-6-diamidino-2-phenylindole (DAPI, Sigma Aldrich). Cells were then studied under a Carl Zeiss LSM710 confocal fluorescence microscope.

Cell Study by SEM. After being cultured for 48 h, the cells were first fixed with 2.5% w/v glutaraldehyde (Sigma) in sodium cacodylate buffer (pH 7.4), then dehydrated using a gradient of ethanol and isoamyl acetate (Sigma). Then, the samples were dried using a critical point drying (CPD) technique using a Bal-Tec 030 instrument. After that, the samples were coated with gold by sputtering and examined with field emission scanning electron microscopy (FE-SEM; Hitachi S-4800).

RESULTS AND DISCUSSION

Characterization of the GaN NWs. The GaN NWs were fabricated by the CVD technique. The morphology of the GaN NWs was examined using scanning electron microscopy (SEM). A typical SEM image (Figure 1A) exhibits a network of NWs with a diameter about 50 nm over the whole substrate. The wettability was evaluated by the water contact angle (CA) measurement of the GaN NWs. The inset of Figure 1A shows the shape of a water droplet (about 5 μL in volume) on GaN NWs with a CA of about 155.0 ± 0.4°, indicating superhydrophobic properties.

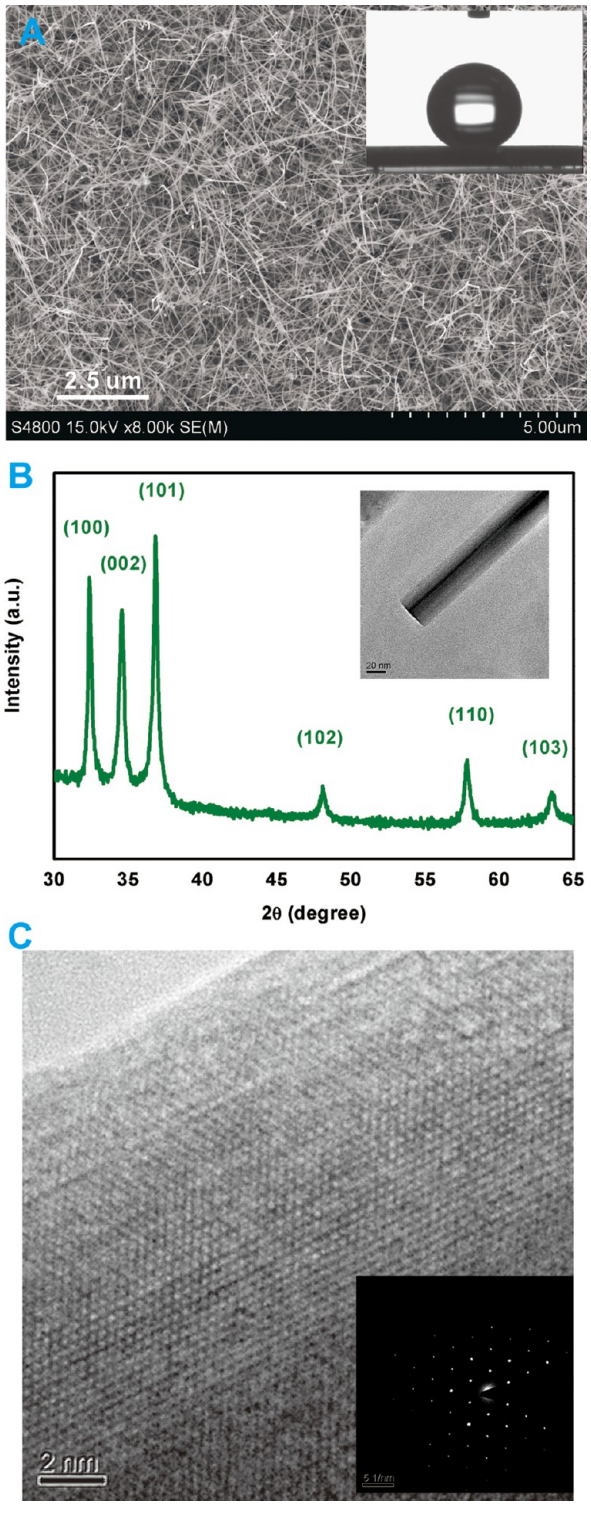

Figure 1. (A) SEM image of GaN nanowires prepared by CVD and the shape of a water droplet on a GaN nanowire film with CA of 155.0°; (B) XRD patterns of GaN nanowires. Inset is a low resolution TEM image of a single GaN NW. (C) High resolution TEM image of a GaN nanowire and corresponding SAED pattern (inset).

X-ray diffraction pattern of the GaN NWs is shown in Figure 1B. All the reflection peaks of 32.4°, 34.6 °, 36.8°, 48.1°, 57.8°, and 63.5° can be ascribable to GaN with the hexagonal wurtzite structure (PDF: 50-0792), indicating the high purity and crystallinity of the products. The structure of a single GaN nanowire was analyzed by transmission electron microscopy and select-area electron diffraction, as shown in Figure 1C. The GaN nanowire is uniform along the growth direction. The corresponding selective area electron diffraction pattern (SAED) along GaN [0001] axis indicates that the growth direction of the nanowire is along $[01\bar{1}0]$.

The as-prepared GaN NW surface is superhydrophobic with a water CA of 155.0 ± 0.4° as shown in Figure 2A (left). Upon UV irradiation for 60 min, the water droplet spread out on the surface and the CA of the film changed to 0° (Figure 2A, right). These results show that the wettability changes from superhydrophobicity to superhydrophilicity. After the film was stored in dark or heated, the surface of the film returned into superhydrophobic again.

To study the wettability switching mechanism, XPS was used to quantify element ratio changes before and after UV illumination. Figure 2, parts B and C, shows the Ga 3d, and N1s XPS spectra of GaN NWs. Before UV irradiation, the Ga 3d peak only composed as single component at ~20 eV, which was indexed to Ga−N bonding.[45,46] After UV treatment, the Ga 3d peak can be decomposed to two components: one around 20 eV and the other one at ~21.3 eV. The latter one is indexed to Ga−O (or Ga−OH) bonding. Meanwhile, the N1s peak is also decomposed into two parts at 397.5 and 399 eV after UV illumination. The former is indexed to N−Ga bonding, and the latter is due to N−O bonding.[46] Element atom ratios were calculated from the element intensities, as shown in Table 1. We found that the UV treatment increased the oxygen to gallium ratio and slightly decreased the N/Ga ratio. Thus, the XPS analyses showed that the UV irradiation resulted in the more oxygen or water molecules adsorption on GaN NW surface.

As is known, UV irradiation can produce electron−hole pairs in semiconductor materials. The electron and hole generated by UV irradiation will move to the GaN NW surface and lead to the formation of vacancies on the surface. Water molecules may easily go into the vacancy sites, resulting in the increase of the water adsorption. As a result, the surface hydrophilicity is improved.

Optical Regulation of Protein Adsorption. One of the important factors to evaluate the biocompatibility and bioactivity of materials is the protein adsorption ability.[47,48] The photosensitive superhydrophobic GaN NW surface is a good model system to investigate the correlation between changes in wettability and the protein adsorption behaviors. We studied the UV illumination related wettability conversion of the GaN NWs and subsequent BSA adsorption.

Figure 3A is the water CAs of the GaN NWs as a function of UV irradiation time under ambient conditions. The contact angle of the GaN NWs declines with UV irradiation. After 20, 30, 40, and 60 min UV irradiation, CA is reduced to 120°, 60°, 20°, and 0°, respectively. After over 60 min UV irradiation, CA showed ~0° and the surface became superhydrophilic.

Figure 3B shows the BSA amounts adsorbed on GaN NW surfaces with different wettabilities, which were created upon different time of UV exposure. The BSA adsorption was determined by BCA assay. From Figure 3B, one can see that the BSA adsorption rate reduces along with the decrease of the CA of GaN NWs after UV irradiation. This declining trend of BSA adsorption with the increase of the surface hydrophilicity is consistent with previous reports.[49−53]

In this GaN/protein nano/biosystem, we investigated the correlation between the changes in wettability without

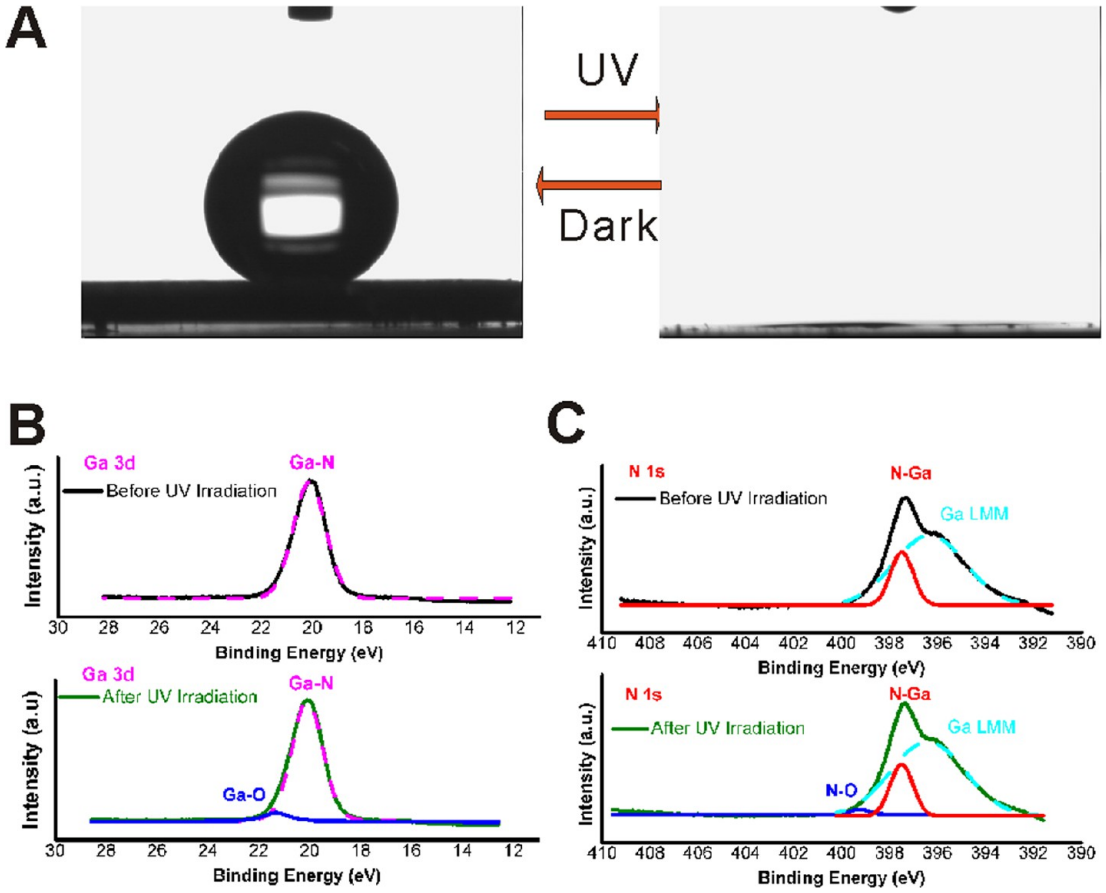

Figure 2. (A) Photos of water droplet on the GaN NWs before and after UV illumination. (B) Ga3d and (C) N1s XPS spectra of GaN NWs before and after UV irradiation.

Table 1. O/Ga and N/Ga Ratios of GaN NW Surfaces before and after UV Illumination

	before UV illumination	after UV illumination
O/Ga ratio	0.508	0.5655
N/Ga ratio	1.275	1.2628

topographical variation and protein adsorption behaviors. In addition, the influence of roughness effect on protein adsorption was also analyzed. Figure 4 shows the comparison of BSA adsorbed quantities on GaN flat and NW surfaces before and after 60 min UV illumination. One can see that the amount of BSA adsorbed on GaN NW surface is higher than that on flat GaN surface before and after UV illumination. The increased surface-to-volume ratio of the nanowires may have contributed to the observed increase in the BSA adsorption. Figure 4 also shows that the magnification effect of nanostructures on wettability of GaN NW surface would also increase the change of protein adsorption.

It could be proposed that the mechanism of modulating the BSA adsorption via introduction of UV light is possibly correlated with the change of the surface wettability, thus the variation of hydrophobic interactions between BSA and GaN surface. Before UV irradiation, the micro/nanostructures of GaN NWs created a superhydrophobic surface. The high adsorption rate of BSA was observed due to the hydrophobic interactions between BSA and the superhydrophobic surface. After UV irradiation, the superhydrophilic surface is formed (CA = 0°). The loss of hydrophobic interactions between BSA and GaN NWs causes desorption of BSA.

Modulation Effects on Cell Adhesion. To study the effect of the properties of GaN nanostructures on cell adhesion, the acridine orange labeled NIH 3T3 and SH-SY5Y cells were studied under a fluorescence microscope. Cells were cultured on two different surfaces (GaN NW surface before and after UV irradiation) for 48 h. Figure 5 shows the fluorescence microscopy images of NIH 3T3 and SH-SY5Y cells on these two surfaces with different wettabilities. On the super-hydrophobic GaN NW surface (Figure 5A, E), only a small amount of cells were adhered, indicating that the super-hydrophobic substrate was not suitable for cell adhesion and proliferation. On the UV treated GaN superhydrophilic surface (Figure 5B, F), more cells were observed, indicating that surface with higher wettability had a favorable impact on the adhesion behavior of the cells.

To investigate the cell morphologies on GaN NW surfaces before and after UV illumination, we performed SEM studies on NIH 3T3 and SH-SY5Y cells. The cells on GaN NWs before UV illumination had a round morphology (Figure 5C, G). On the GaN surface after UV illumination, cells exhibit flatter and more-extended morphologies (Figure 5D, H). The elongated filopodia of the cells closely touched with the nanowires. The size of the cells was larger compared to that on the surface before UV illumination.

Figure 6 is the ratio of the number of cells on GaN NWs before UV irradiation to that on GaN NW surface after UV irradiation for NIH 3T3 and SH-SY5Y cells. The number of

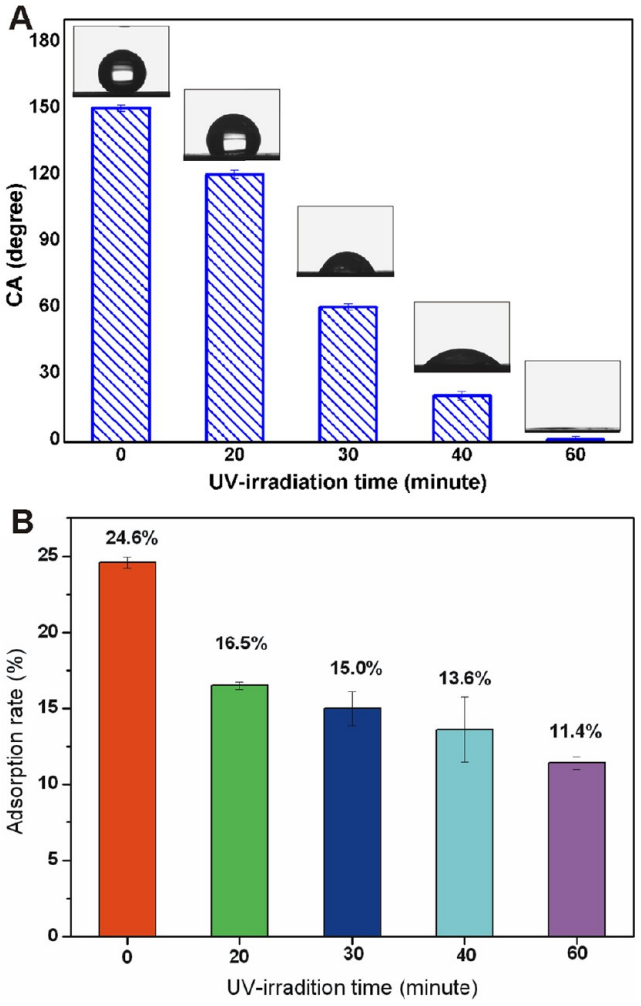

Figure 3. Evaluation of the surface wettability and the corresponding adsorption of BSA. (A) CA as a function of UV irradiation time for the GaN NWs. (B) BSA adsorption rate on GaN NW surface with different wettabilities which were created by different UV illumination time.

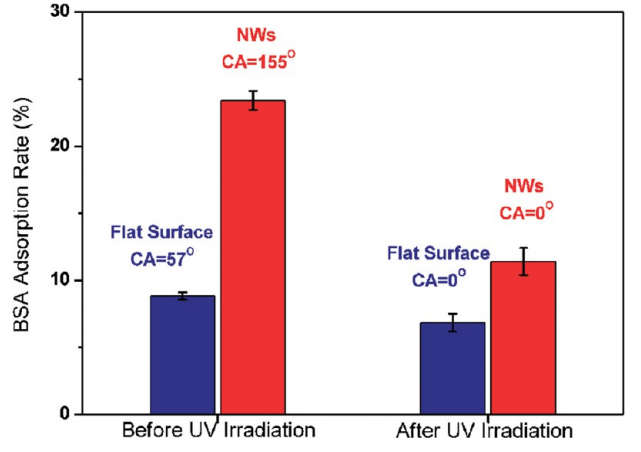

Figure 4. Comparison of BSA adsorption rates on GaN flat and NW surfaces before and after 60 min UV irradiation.

cells on GaN NWs before UV irradiation was significantly lower than that on the surface after UV irradiation for both cell types. Our results indicate that the wettability can profoundly modulate cell behavior.

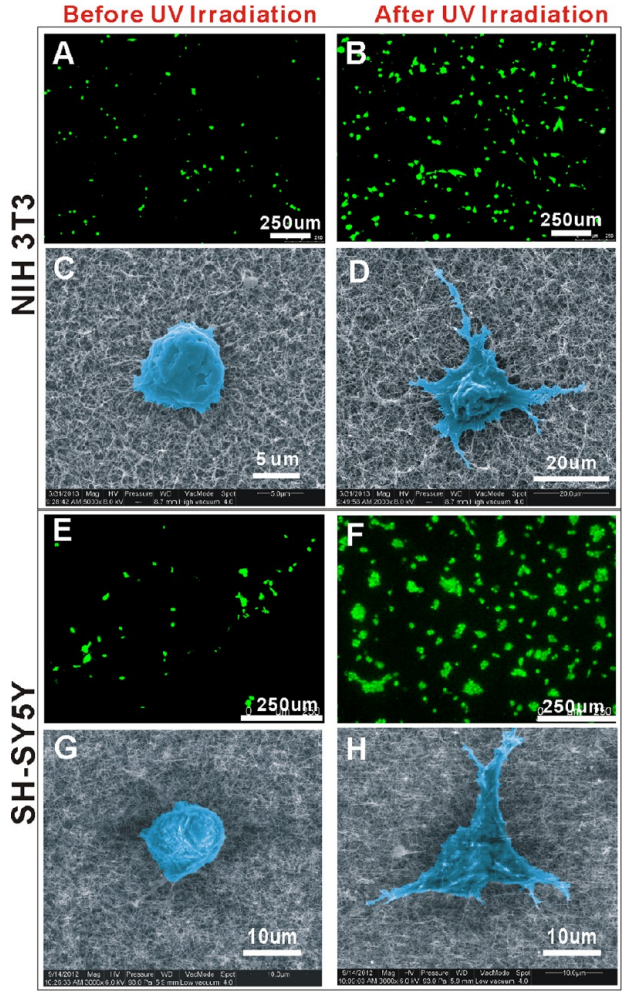

Figure 5. Fluorescence microscopy images and SEM images of cells cultured for 48 h on GaN NW surfaces before and after UV irradiation. (A–D) NIH 3T3 cells; (E–H) SH-SY5Y cells.

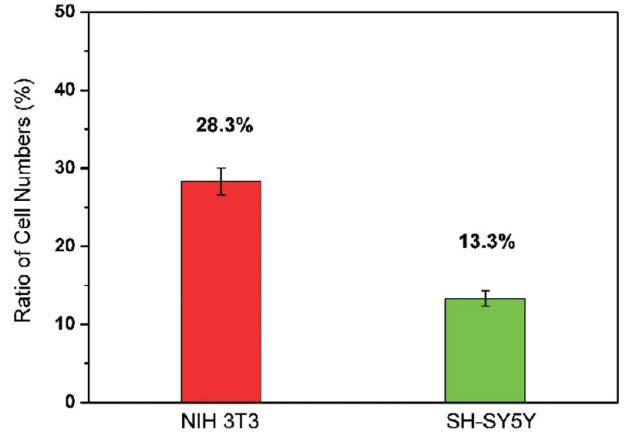

Figure 6. Ratio of the number of cells on GaN NW surface before UV irradiation to that on GaN NW surface after UV irradiation.

As is known, the cell attachment and spreading on surfaces are mediated by focal adhesion, a multiprotein assembly that mediates the cell–substrate adhesion. If focal adhesions cannot assemble in cells, the cell–substrate interactions will be weak.[54] Therefore, the assembly of focal adhesions was next studied using immunofluorescence microscopy.

Figure 7 shows fluorescence images of NIH 3T3 cells on GaN NW surfaces before and after UV irradiation. Cells

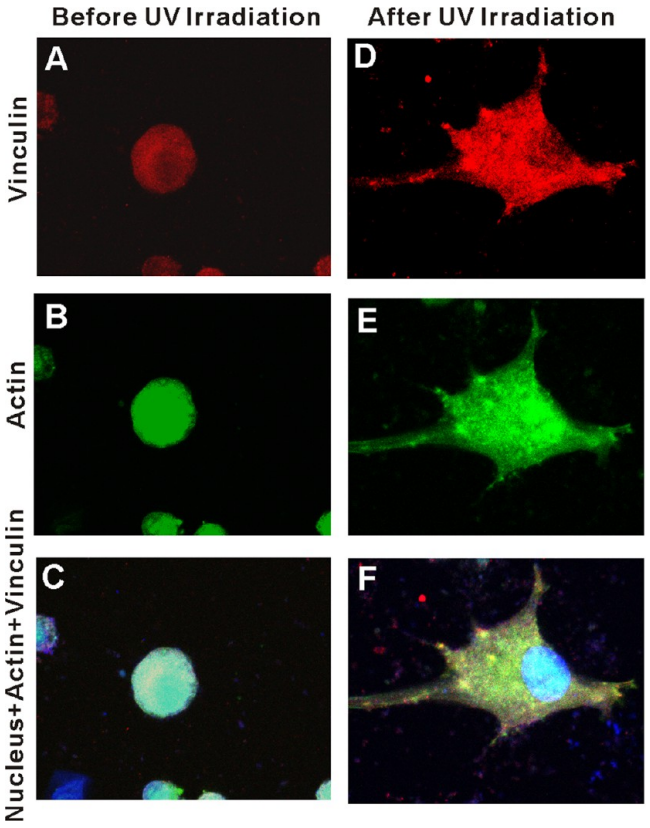

Figure 7. Confocal images of NIH 3T3 cells. The cells stained for vinculin (red), actin (green), and nucleus. All cells cultured for 48 h on GaN NW surfaces before (A–C) and after (D–F) UV irradiation. Triple stained images are also shown.

cultured on GaN NWs were stained for vinculin, actin, and the nucleus. The high expression of vinculin will indicate the existence of strong cell–substrate adhesion.[54] On the GaN NWs before UV irradiation, focal adhesions could not be visible and cells were round and poorly spread (Figure 7A–C). This result suggested that the superhydrophobicity of that surface resulted in decreased formation of actin stress fibers and focal adhesions. The low vinculin expression indicates the weak cell–substrate adhesion on superhydrophobic surface.[54] On the other hand, it is clearly observed that cells assembled vinculin labeled focal adhesions on the NW surface after UV irradiation (Figure 7D–F).

On the basis of the above results, a schematic illustration is proposed in Figure 8 showing the effect of optical regulation on the cell adhesion. On as-prepared superhydrophobic GaN NWs, cells will adhere mostly to some points of the nanostructure surface, inducing the cells to have a round shape. Upon UV irradiation, the superhydrophilic surface is obtained, which may achieve more efficient adhesion by enhanced cell–substrate interactions. Thus, the GaN NW surfaces can be switched from cell-repellent to cell-attractive.

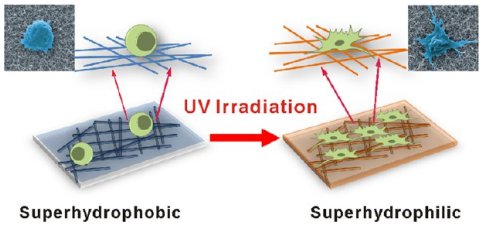

Figure 8. Schematic illustration of cell morphologies on GaN NW surfaces before and after UV illumination.

CONCLUSIONS

In summary, large-scale photoresponsive superhydrophobic GaN NWs were successfully fabricated by the CVD method. The optical regulation effects of the GaN NWs on BSA adsorption were investigated. The tunable cell adhesion was also observed. The experimental results show that the combination of the photoresponsive GaN surface and the magnification effect of micro/nanostructures resulted in a large-scale change of surface wettability from superhydrophobicity to superhydrophilicity by UV light stimuli, which subsequently modulated the protein adsorption and cell adhesion. This provides an important insight into the design of novel high-performance smart stimuli-responsive biointerface materials. The nonfouling properties of superhydrophobic GaN NW surface may lead to novel and promising applications such as the improvement of biocompatibility in medical implants, where devices are prone to contamination; the greatly increased cell adhesion on superhydrophilic GaN NW surface will provide a useful platform to probe and manipulate the cell behaviors. The formation of tight interfaces between NWs and cells would lend promise for monitoring and/or stimulating of cells. These findings may open new avenues for the design of GaN NW-based, advanced functional devices for cell culture engineering, bioseparation, and diagnostics.

AUTHOR INFORMATION

Corresponding Authors

*E-mail: yangr@nanoctr.cn .

*E-mail: wangch@nanoctr.cn.

Author Contributions

‖J.L. and Q.H. contributed equally.

Notes

The authors declare no competing financial interest.

ACKNOWLEDGMENTS

This work was supported by National Natural Science Foundation of China (21073047, 21261130090, 11174042, and 11374039) and the National Basic Research Program of China (973 Program) (2011CB922204). Financial support from CAS Key Laboratory of Biological Effects of Nanomaterials and Nanosafety is also gratefully acknowledged.

REFERENCES

(1) Xie, C.; Lin, Z.; Hanson, L.; Cui, Y.; Cui, B. *Nat. Nanotechnol.* **2012**, *7*, 185–190.

(2) Nguyen, T. D.; Deshmukh, N.; Nagarah, J. M.; Kramer, T.; Purohit, P. K.; Berry, M. J.; McAlpine, M. C. *Nat. Nanotechnol.* **2012**, *7*, 587–593.

(3) Bucaro, M. A.; Vasquez, Y.; Hatton, B. D.; Aizenberg, J. *ACS Nano* **2012**, *6*, 6222–6230.

(4) Peer, E.; Artzy-Schnirman, A.; Gepstein, L.; Siva, U. *ACS Nano* **2012**, *6*, 4940–4946.

(5) Du, K.; Gan, Z. *ACS Appl. Mater. Interfaces* **2012**, *4*, 4643–4650.

(6) Kwiat, M.; Elnathan, R.; Pevzner, A.; Peretz, A.; Barak, B.; Peretz, H.; Ducobni, T.; Stein, D.; Mittelman, L.; Ashery, U.; Patolsky, F. *ACS Appl. Mater. Interfaces* **2012**, *4*, 3542–3549.

(7) Kim, W.; Ng, J. K.; Kunitake, M. E.; Conklin, B. R.; Yang, P. *J. Am. Chem. Soc.* **2007**, *129*, 7228−7229.
(8) Krivitsky, V.; Hsiung, L.; Lichtenstein, A.; Brudnik, B.; Kantaev, R.; Elnathan, R.; Pevzner, A.; Khatchtourints, A.; Patolsky, F. *Nano Lett.* **2012**, *12*, 4748−4756.
(9) Qi, S.; Yi, C.; Ji, S.; Fong, C.; Yang, M. *ACS Appl. Mater. Interfaces* **2009**, *1*, 30−34.
(10) Yang, P.; Yan, R.; Fardy, M. *Nano Lett.* **2010**, *10*, 1529−1536.
(11) Piret, G.; Galopin, E.; Coffinier, Y.; Boukherroub, R.; Legrandc, D.; Slomiann, C. *Soft Mater.* **2011**, *7*, 8642−8649.
(12) Lee, K.; Shim, S.; Kim, I.; Oh, H.; Kim, S.; Ahn, J.; Park, S.; Rhim, H.; Choi, H. *Nanoscale Res. Lett.* **2010**, *5*, 410−415.
(13) Hällström, W.; Mårtensson, T.; Prinz, C.; Gustavsson, P.; Montelius, L.; Samuelson, L.; Kanje, M. *Nano Lett.* **2007**, *7*, 2960−2965.
(14) Patolsky, F.; Timko, B. P.; Yu, G.; Fang, Y.; Greytak, A. B.; Zheng, G.; Lieber, C. M. *Science* **2006**, *313*, 1100−1104.
(15) Berthing, T.; Bonde, S.; Soensen, C. B.; Utko, P.; Nygard, J.; Martinez, K. L. *Small* **2011**, *7*, 640−647.
(16) Stern, E.; Klemic, J. F.; Routenberg, D. A.; Wyrembak, P. N.; Turner-Evans, D. B.; Hamilton, A. D.; LaVan, D. A.; Fahmy, T. M.; Reed, M. A. *Nature* **2007**, *445*, 519−522.
(17) Kotov, N. A.; O. Winter, J.; Clements, I. P.; Jan, E.; Timko, B. P.; Campidelli, S.; Pathak, S.; Mazzatenta, A.; Lieber, C. M.; Prato, M.; Bellamkonda, R. V.; Silva, G. A.; Kam, N. W. S.; Patolsky, F.; Ballerini, L. *Adv. Mater.* **2009**, *21*, 3970−4004.
(18) Qing, Q.; Pal, S. K.; Tian, B.; Duan, X.; Timko, B. P.; Cohen-Kami, T.; Murthy, V. N.; Lieber, C. M. *Proc. Natl. Acad. Sci.* **2010**, *107*, 1882−1887.
(19) Xie, C.; Cui, Y. *Nano Lett.* **2010**, *10*, 4020−4024.
(20) Huang, Y.; Duan, X.; Cui, Y.; Lieber, C. M. *Nano Lett.* **2002**, *2*, 101−104.
(21) Kuykendall, T.; Pauzauskie, P.; Lee, S.; Zhang, Y.; Goldberger, J.; Yang, P. *Nano Lett.* **2003**, *3*, 1063−1066.
(22) Johnson, J. C.; Choi, H. J.; Knutsen, K. P.; Schaller, R. D.; Yang, P.; Saykally, R. J. *Nat. Mater.* **2002**, *1*, 106−110.
(23) Zhong, Z.; Qian, F.; Wang, D.; Lieber, C. M. *Nano Lett.* **2003**, *3*, 343−346.
(24) Qian, F.; Li, Y.; Gradecak, S.; Park, H. G.; Dong, Y.; Ding, Y.; Wang, Z. L.; Lieber, C. M. *Nat. Mater.* **2008**, *7*, 701−706.
(25) Huang, C.; Song, J.; Lee, W.; Ding, Y.; Gao, Z.; Hao, Y.; Chen, L.; Wang, Z. L. *J. Am. Chem. Soc.* **2010**, *132*, 4766−4771.
(26) Kang, B. S.; Wang, H. T.; Lele, T. P.; Tseng, Y.; Ren, F.; Pearton, S. J.; Johnson, J. W.; Rajagopal, P.; Roberts, J. C.; Piner, E. L.; Linthicum, K. *J. Appl. Phys. Lett.* **2007**, *91*, 112106−1−3.
(27) Chen, C.; Young, T. *Biomaterials* **2008**, *29*, 1573−1582.
(28) Chen, C.; Ganguly, A.; Wang, C.; Hsu, C.; Chattopadhyay, S.; Hsu, Y.; Chang, Y.; Chen, K.; Chen, L. *Anal. Chem.* **2009**, *81*, 36−42.
(29) Gebinoga, M.; Mai, P.; Donahue, M.; Kittler, M.; Cimalla, I.; Lubbers, B.; Klett, M.; Lebedev, V.; Silveira, L.; Singh, S.; Schober, A. *J. Neurosci. Meth.* **2012**, *206*, 195−199.
(30) Jewett, S. A.; Makowski, M. S.; Andrews, B.; Manfra, M. J.; Ivanisevic, A. *Acta Biomaterialia* **2012**, *8*, 728−733.
(31) Young, T. H.; Chen, C. R. *Biomaterials* **2006**, *27*, 3361−3367.
(32) Chen, C. R.; Li, Y. C.; Young, T. H. *Biomaterials* **2009**, *5*, 2610−2617.
(33) Chen, C. R.; Young, T. H. *Biomaterials* **2008**, *29*, 1573−1582.
(34) Ganguly, A.; Chen, C.; Lai, Y.; Kuo, C.; Hsu, C.; Chen, K.; Chen, L. *J. Mater. Chem.* **2009**, *19*, 928−933.
(35) Michiardi, A.; Aparicio, C.; Ratner, B. D.; Planell, J. A.; Gil, J. *Biomaterials* **2007**, *28*, 586−594.
(36) Benoit, D. S. W.; Schwartz, M. P.; Durney, A. R.; Anseth, K. S. *Nat. Mater.* **2008**, *7*, 816−823.
(37) Lim, J. Y.; Shaughnessy, M. C.; Zhou, Z. Y.; Noh, H.; Vogler, E. A.; Donahue, H. J. *Biomaterials* **2008**, *29*, 1776−1784.
(38) Song, W.; Veiga, D. D.; Custódio, C. A.; Mano, J. F. *Adv. Mater.* **2009**, *21*, 1830−1834.
(39) Neto, I.; Custódio, C. A.; Song, W.; Mano, J. F. *Soft Matter* **2011**, *7*, 4147−4151.
(40) Ueda, E.; Levkin, P. A. *Adv. Mater.* **2013**, *25*, 1234−1247.
(41) Song, W.; Mano, J. F. *Soft Mater.* **2013**, *9*, 2985−2999.
(42) Dolatshahi-Pirouz, A.; Jensen, T.; Kraft, D. C.; Foss, M.; Kingshott, P.; J. Hansen, L.; Larsen, A. N.; Chevallier, J.; Besenbacher, F. *ACS Nano* **2010**, *4*, 2874−2882.
(43) Lee, J.; Chu, B. H.; Chen, K.; Ren, F.; Lele, T. P. *Biomaterials* **2009**, *30*, 4488−4493.
(44) Liu, L.; Zhang, L.; Niu, L.; Xu, M.; Mao, X.; Yang, Y.; Wang, C. *ACS Nano* **2011**, *5*, 6001−6007.
(45) Zhang, L. Q.; Zhang, C. H.; Gou, J.; Han, L. H.; Yang, Y. T.; Sun, Y. M.; Jin, Y. F. *Nucl. Instrum. Methods Phys. Res., Sect. B* **2011**, *269*, 2835−2839.
(46) Kida, T.; Minami, Y.; Guan, G.; Nagano, M.; Akiyama, M.; Yoshida, A. *J. Mater. Sci.* **2006**, *41*, 3527−3534.
(47) Ayala, R.; Zhang, C.; Yang, D.; Hwang, Y.; Aung, A.; Shroff, S. S.; Arce, F. T.; Lal, R.; Arya, G.; Varghese, S. *Biomaterials* **2011**, *32*, 3700−3711.
(48) Du, K.; Gan, Z. *ACS Appl. Mater. Interfaces* **2012**, *4*, 4643−4650.
(49) Lampin, M.; Warocquier, C.; Legris, C.; Degrange, M.; Sigot-Luizard, M. F. J. *Biomed. Mater. Res* **1997**, *36*, 99−108.
(50) Lindman, S.; Lynch, I.; Thulin, E.; Nilsson, H.; Dawson, K. A.; Linse, S. *Nano Lett.* **2007**, *7*, 914−920.
(51) Mueller, C.; Lueders, A.; Hoth-Hannig, W.; Hannig, M.; Ziegler, C. *Langmuir* **2010**, *26*, 4136−4141.
(52) Trudeau, T. G.; Hore, D. K. *Langmuir* **2010**, *26*, 11095−11102.
(53) Ishihara, K.; Kyomoto, M. *J. Photopoly. Sci. Technol.* **2010**, *23*, 161−166.
(54) Lee, J.; Chu, B. H.; Chen, K. H.; Ren, F.; Lele, T. P. *Biomaterials* **2009**, *30*, 4488−4493.